

Presented at the 9th International
Congress on Electron Microscopy,
Toronto, Canada, August 1-9, 1978

LBL-7677

c.j.

ADVANCES IN CHARACTERIZATION OF MATERIALS:
ALLOYS AND CERAMICS

Gareth Thomas

RECEIVED
LAWRENCE
BERKELEY LABORATORY

AUG 22 1978

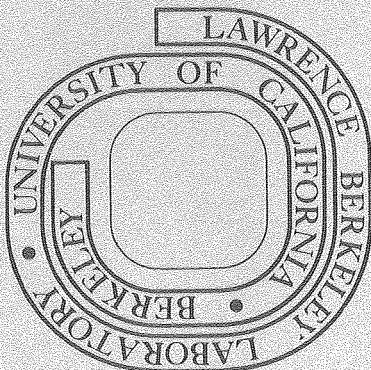
May 1978

LIBRARY AND
DOCUMENTS SECTION

Prepared for the U. S. Department of Energy
under Contract W-7405-ENG-48

TWO-WEEK LOAN COPY

*This is a Library Circulating Copy
which may be borrowed for two weeks.
For a personal retention copy, call
Tech. Info. Division, Ext. 6782*



LBL-7677
c.j.

This report was done with support from the Department of Energy. Any conclusions or opinions expressed in this report represent solely those of the author(s) and not necessarily those of The Regents of the University of California, the Lawrence Berkeley Laboratory or the Department of Energy.

ADVANCES IN CHARACTERIZATION OF MATERIALS:
ALLOYS AND CERAMICS

Gareth Thomas

Department of Materials Science and Mineral Engineering, College
of Engineering, and Materials and Molecular Research Division,
Lawrence Berkeley Laboratory, University of California,
Berkeley, California 94720

1. Introduction

The properties of materials are structure-sensitive. Structure is in turn determined by composition, heat-treatment and processing. Thus it is necessary to characterize both composition and microstructure at the highest levels of resolution possible in order to understand materials behavior. Such characterization requires advanced and sophisticated methods of analysis using microscopic, diffraction and spectroscopic techniques. For this of course electron microscopy is particularly versatile, since we are now routinely synthesizing structure almost at atomic levels of resolution. The interaction between composition, heat treatment and properties is complex but this interaction must be understood if materials are to be improved or new materials to be designed.

Figure 1 shows a schematic indicating the important role that electron microscopy now plays in research in materials science and engineering (e.g., failure analysis). The problem solving approach is not limited to a single technique and it is not implied that electron microscopy can solve all problems but clearly the method is very powerful. For certain applications high voltage microscopy shows a great expansion in the type of materials that can be studied¹ due to its advantages² with regard to ionisation damage and improved resolution both in imaging and diffraction). For all applications composition analysis by spectroscopy³ and high resolution lattice parameter measurements⁴ is essential. The new analytical instruments with microdiffraction and X-ray and electron energy loss microanalytical capabilities are welcome additions to the materials scientists "bag of tools" as these methods offer large gains in spatial resolution compared to more conventional analytical methods.

In this review I will draw on examples from some of the current research programs going on in my group, with particular emphasis on high resolution methods, including lattice imaging and microanalysis. For close-packed structures as is common in metals and alloys and many ceramics, point resolutions better than about 2Å are needed for structure imaging and with present day instruments this is not yet possible. Thus we are limited to lattice imaging for HREM studies of these materials. The researchers involved are acknowledged at the appropriate places in this paper and I express my gratitude to them for their assistance.

2. Metallic Alloys

A. Morphology, Crystallography and Formation of Dislocated Lath Martensites in Steels, (B. V. N. Rao)

Although the morphology and crystallography of plate martensites are well understood, the same is not true for the dislocated "lath" martensite occurring in the technologically more important medium and low C steels. A detailed electron diffraction and microscopy examination of dislocated lath martensites has been undertaken partly stimulated by the detection through careful dark-field analysis of small amounts of retained austenite in many lath martensites during an extensive alloy design program on dislocated martensitic steels⁵. Consequently, the unique orientation relationships can be obtained directly by utilizing selected area diffraction analysis of the lath bundles and the surrounding austenite. The present discussion will be limited to results on binary Fe-Ni alloys (Table 1).

Table 1

Chemistry of the alloys and their M_s structures

Alloy #	Alloy Comp. (wt%), Nomial	M_s (°C)
1)	Fe-12 Ni	300*
2)	Fe-15 Ni	250*
3)	Fe-20 Ni	165*

*calculated

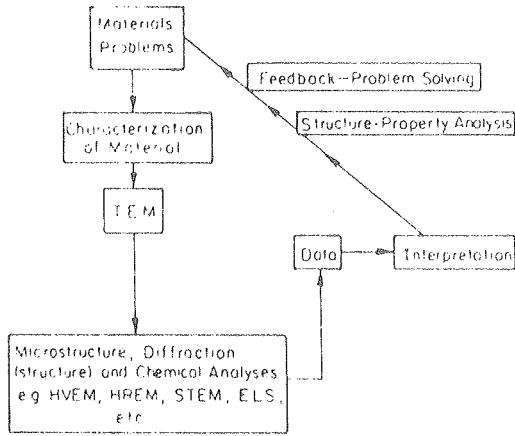
Morphology and Cell Structure of Martensite

The martensite packet size was found by optical microscopy to increase with austenitizing temperature and prior austenite grain size, although there was no similar variation in the average lath width. Therefore, the aspect ratio of the laths increases with prior austenite grain size. A constant aspect ratio with increasing packet size would result in a higher volume dependent strain energy. Transmission electron micrographs taken at 100 kV and 500 kV (Fig. 2(a)) revealed that the laths are parallel with reasonably straight boundaries and a high dislocation density. Although there were no significant differences in lath morphology or substructure as a function of carbon content, retained austenite could only be detected in carbon containing alloys. The advantages of using 500 kV are in the increased accuracy of selected area diffraction for the analyses described below. Knock-on damage is negligible at this voltage.

Relative Orientation of Adjacent Laths

Figure 2 is an example of the detailed analysis of parallel "laths" in the packet martensite. The SAD patterns (Fig. 2(b)) and regions from where the patterns were obtained in the bright field image (Fig. 2(a)) are identified by 1, 2, 3. The $[110]_{\alpha}$ crystal direction remains parallel in all the laths in this packet indicating that these laths are separated by $[110]$ rotation boundaries. Fig. 3 shows a typical stereographic analysis of relative orientations of adjacent laths of a packet in these binary Fe-Ni alloys. From Fig. 3, it was found that lath 5 is rotated 180° with respect to lath 1 indicating that the shear components are opposite and accommodative. The present observations suggest that the orientation of the laths in a given packet are those that result from minimization of the overall shape deformation and its accommodation over a group of laths. Our work also shows that a gradual change in orientation to minimize shape deformation is preferred to a twin orientation of the adjacent laths, although the tendency for the latter increases with carbon content. It is suggested that the austenite-martensite interface may be a ledge boundary and that the macroscopic and microscopic habit planes could be different. It is also concluded that the martensite laths are indeed thin platelets and that individual laths and not the packets are the fundamental nucleation events.

In order to prove these suggestions lattice imaging techniques are being utilized to analyse the austenite-martensite interfaces. These experiments are extremely



XBL 785-5018
FIG. 1

FIG. 1
Schematic showing role of electron microscopy in materials research.

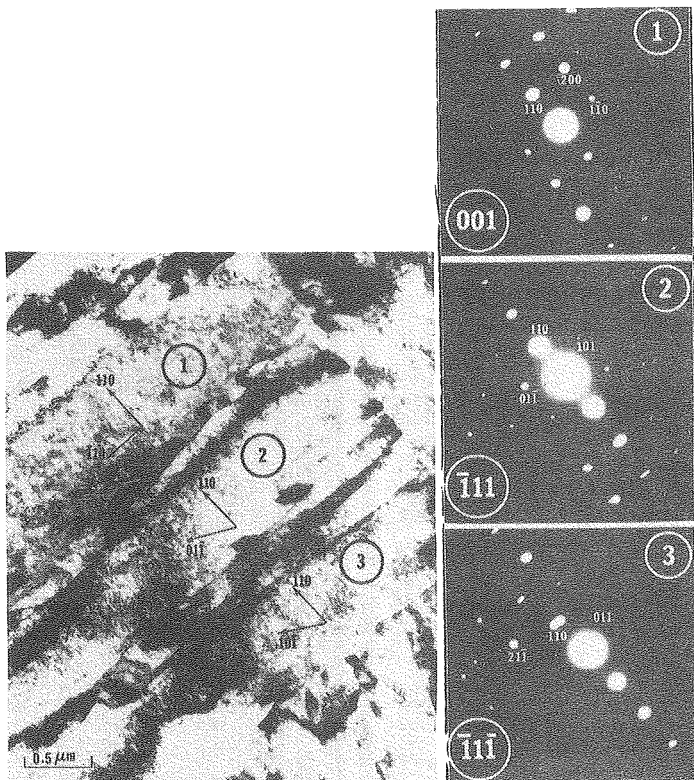
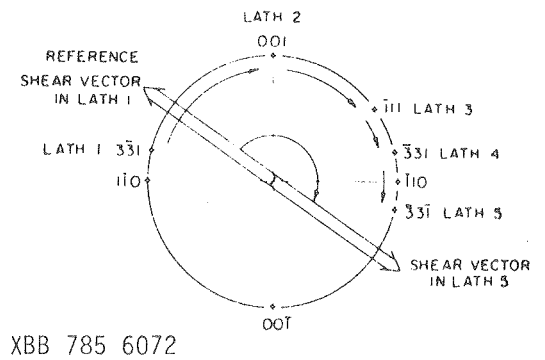


FIG. 2(a) XBB 785 6071
500 kV Bright field images of a packet of dislocated martensite in Fe-15%Ni.

FIG. 2(b)
Selected area diffraction patterns from the laths indicated in the packet of Fig. 2(a).



XBB 785 6072

LATH REGION		ROTATION (DEGREES)
FROM	TO	
1	2	76.75
2	3	54.71
3	4	22.01
4	5	26.53
		180 TOTAL

FIG. 3
XBL 7710 6265
FIG. 3
Typical stereographic projection of orientation amongst laths in a packet of binary Fe-Ni alloys: notice rotation of adjacent laths.

difficult due to the astigmatism corrections (martensite is magnetic, austenite is not). Measurements of fringe spacings in 101 planes also enable carbon contents to be estimated. Such analysis is not possible by X-ray STEM microanalysis.

B. Grain Boundaries and Grain Boundary Precipitation (Al-Zn Alloys), (R. Gronsky)

The ability to detect highly localized compositional variations is a very desirable characteristic for experimental studies of grain boundaries. In current analysis of grain boundary precipitation reactions⁷ we have used lattice imaging, from which fringe spacing measurements have given clear indications of composition profiles in the grain boundary vicinity with high precision. These results have been useful in identifying the involved reaction mechanisms and the particular role of grain boundaries in the precipitation processes.

Fig. 4 is an example of a lattice image of a grain boundary precipitate in an Al-9.5 at %Zn alloy aged 30 mins. at 180°C. The boxed region in (a) is shown enlarged in (b), indicating the region from which compositional analysis is performed. Fringe spacings were measured within both matrix (M) and precipitate (P) areas, at increasing distances from the grain boundary. The results are presented in Fig. 5, each point indicating the average spacing of ten fringes, with a representative scatter band showing the limits of experimental error.

This plot clearly indicates a decreasing fringe spacing as the boundary (dotted line) is approached from either side. It suggests that a solute gradient exists within both the matrix and the precipitate, and the concentration changes rapidly over a distance of only 50Å. Confirmation of this suggestion awaits application of STEM microanalysis—a capability now being installed on our EM 301 microscope. However one feature revealed by the lattice image method is that the segregation appears to be orientation dependent. Thus the power of combining different techniques is apparent.

C. Spinodal Decomposition, (C. K. Wu)

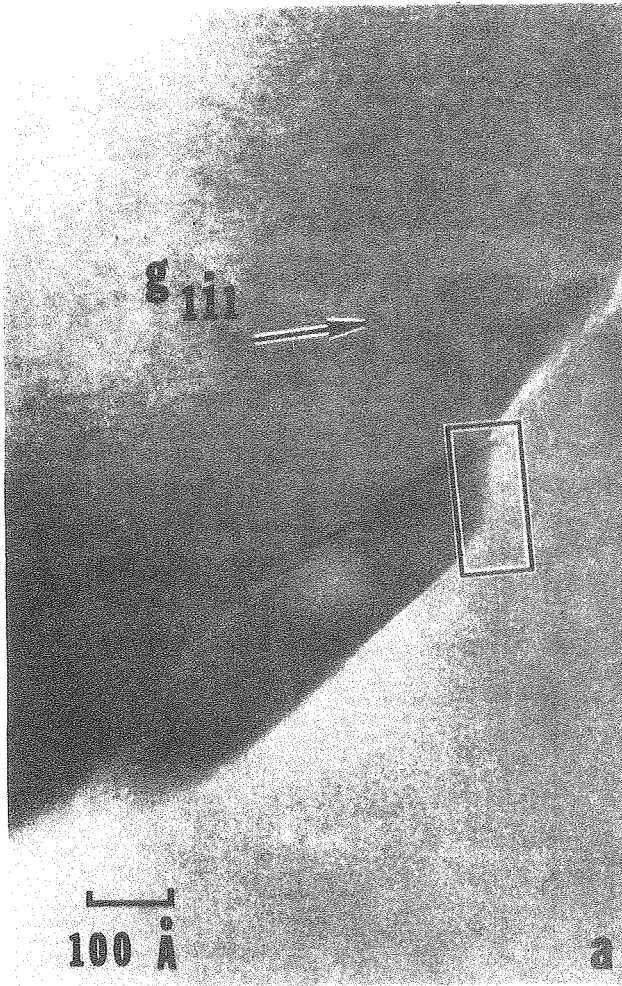
We have had considerable interest in characterizing the morphology of spinodal decomposition by conventional and more recently, high resolution techniques^{4,8}. The latter method using lattice fringe imaging and optical microdiffraction has proven to be extremely useful in analyses of the early stages of the reaction, particularly since the composition variations are very small, and can easily escape detection by familiar imaging or spectroscopic techniques. Thus the variation of lattice parameters with spinodal wavelength down to ~10Å can be determined in this way⁹.

Another application of the lattice imaging method has been the distinction between modes of decomposition in the critical vicinity of the coherent spinodal which is inside the chemical spinodal but which is not known for the Au - Ni system. Figure 6 shows an example for alloys aged near the vicinity of what is expected to be the coherent spinodal. The lattice image (a) clearly distinguishes the "typical" zone segregation whilst, (b) has the sinusoidal periodicity typical of spinodals. A significant result of this research is that the decomposition appears to be one dimensional in the early stages.

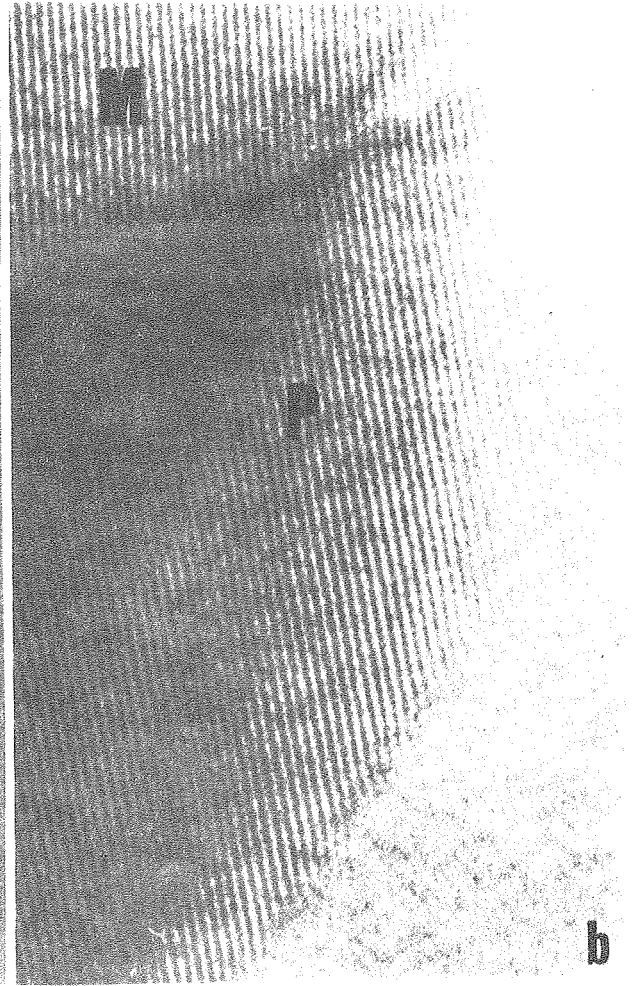
3. Refractory Ceramics - Silicon Nitride and Sialons

A. Intergranular Phases, (O. Krivanek, T. M. Shaw)

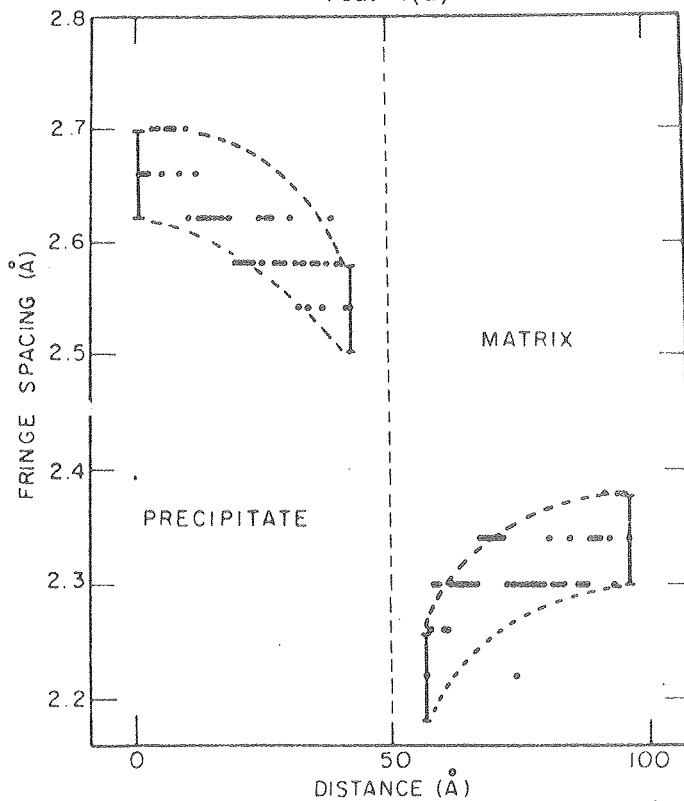
The potential advantages of refractory ceramics for high temperature applications e.g., gas turbines and liquid metal containers are well recognized since they have very attractive properties (high modulus: density ratios, high melting points, oxidation resistance, etc.). However, due to fabrication difficulties the use of hot-pressing additives such as MgO or Y₂O₃, are needed and the properties at high temperatures are impaired. It has been proposed that the impairment is due to the formation of an intergranular phase, probably glassy as a result of the formation of silicates and crystalline oxy nitrides. Attempts to prove this have been successful using high resolution TEM¹⁰. The problem of resolving intergranular phases and whether they are amorphous or not is however not trivial. From an electron microscopy viewpoint therefore, the following features at grain boundaries require characterization: 1) detecting



XBB 7611 10514A
FIG. 4(a)



XBB 7611 10514A
FIG. 4(b)



XBL 7611 7804A
FIG. 5

FIG. 4

(a) Lattice image of a grain boundary precipitate in an Al-9.5 at.% Zn alloy.

(b) Enlargement of boxed region in (a); Matrix images of (111) precipitate (0002 fringes).

FIG. 5

Plot of fringe spacing as a function of distance from the grain boundary in Fig. 4 (dotted line). Each point represents 10 measurements. The data clearly show a gradient in lattice parameter and hence composition.

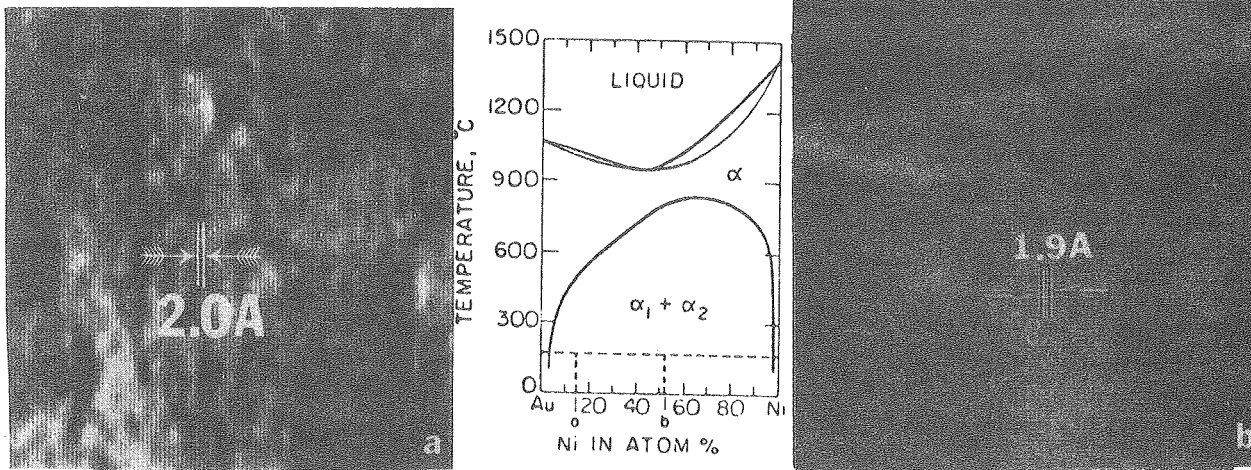


FIG. 6 XBB 7711 11454
 FIG. 6(a)

XBB 7711 11454
 FIG. 6(b)

Lattice imaging of 200 planes in Au-Ni alloys to establish the coherent spinodal. Alloy (a) shows typical G. P. Zones and alloy (b) typical spinodal morphologies. Thus (a) must be outside the coherent spinodal even though it is inside the chemical spinodal (phase diagram in center).

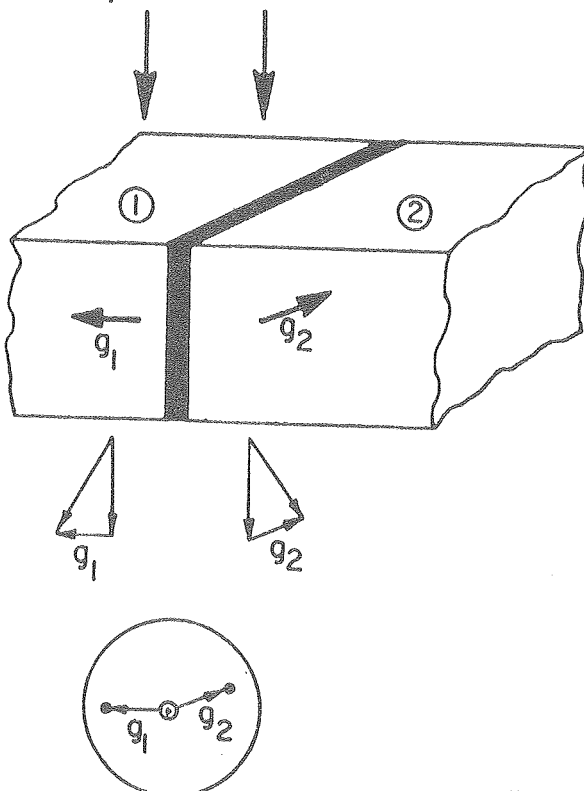


FIG. 7

Necessary contrast conditions for analyzing grain boundary interfaces and for detecting intergranular phases. The boundary must be parallel to the incident beam. The inset shows diffracting conditions for simultaneous lattice imaging in both grain 1 and 2.

FIG. 7

the intergranular phases and their distribution, 2) determining whether these phases are crystalline, and 3) determining their chemical compositions.

From a morphological viewpoint it is essential to choose the proper orientation conditions as sketched in Fig. 7. Under conventional imaging conditions the grain boundary should be viewed edge-on with simultaneous strong Bragg excitation in adjacent grains. The contrast from intergranular phases if present and resolved depend upon whether they are amorphous or crystalline. Amorphous phases (most probably silicates) generally appear in light contrast (low atomic number-mass thickness contrast) as shown in Figs. 8(a) and 9(b). Dark field imaging of the grains, although difficult, is preferable to enhance grain boundary interphase contrast. One can take advantage of the well known ionisation radiation damage sensitivity of glasses in order to detect this phase. At 100 kV, exposure to the electron beam results in such damage and so very quickly it becomes apparent which parts of the microstructure are glassy. Examples are shown in Figs. 8(a) and 8(b). The incoherent scattering from these regions can then be quickly identified by placing the SAD aperture over these regions and locating the area in the diffraction pattern. Dark field analysis of this area reveals the glassy phases as shown in Fig. 8(b). However it is still not certain that all the dark field contrast especially in very narrow intergranular regions can be claimed to be exclusively due to glassy phases. Also these materials are very complex - both the amount and composition of glassy phase varies (e.g., Figs. 8, 10). Images such as in Fig. 8 are not often observed in HS130 or NC 132^{8,9}. Thus the problem of characterization must be done meticulously and with enough samples and areas to be statistically meaningful.

The bright field lattice imaging technique shows the glassy grain boundary phase very directly, but careful experimentation is essential. It has been shown that slight mistilt of the grain boundary away from the edge-on configuration can obscure a 10Å wide glassy phase, and not even a perfect edge-on orientation can guarantee the detection of the phase. This point is illustrated in Fig. 9(a) where a through-focal series of lattice images is shown together with optical diffractograms of the Si₃N₄ image and the amorphous carbon film present on the foil surface. Only the Scherzer defocus image shows the amorphous phase with any clarity, while in the first contrast transfer over focus image the two silicon nitride grains appear to join up. The DF image of this region, on the other hand, shows the glassy phase quite clearly (Fig. 9(b)). The DF approach is thus seen to offer two advantages: defocus and specimen tilt are not very critical, and large areas of the material can be examined at once.

However recent work on Y₂O₃ hot pressed Si₃N₄⁹ has shown that with proper care lattice imaging is a very powerful technique for revealing amorphous phase ~10Å wide between crystalline Si₃N₄ and the yttrium oxynitride. Here again STEM X-ray analysis shows considerable impurity segregation. Thus the composition of the glassy phase which controls its melting point is of critical significance in determining mechanical properties.

Figure 10 shows a BF - DF pair from a Be Sialon prepared by hot-pressing with no additives. The very weak grain boundary lines in the DF image are due to scattering from the intrinsic grain boundary disorder, and there is no glassy phase (within these limits of detectability say ~4Å). This material, closely related to Si₃N₄, is therefore expected to have considerably superior high-temperature mechanical properties.

One of the problems with chemical analysis (spectroscopy) of the sialons is that they contain light elements. Since X-ray analysis is for most practical purposes limited to elements for $Z \geq 11$, electron energy loss spectroscopy becomes particularly important. Qualitatively this point is well illustrated by Fig. 11 taken from the sample shown in Fig. 10.

B. Magnetic Materials: Garnets, (T. Roth)

Calcium Gallium Germanium Garnet (CGGG) can be used as a substrate material for magnetic bubble devices. In such applications a thin magnetic garnet film is grown epitaxially on the substrate. Consequently, defect-free substrate single crystals are desired since inhomogeneities in the substrate can be replicated in the epitaxial film and lead to degradation of device performance.

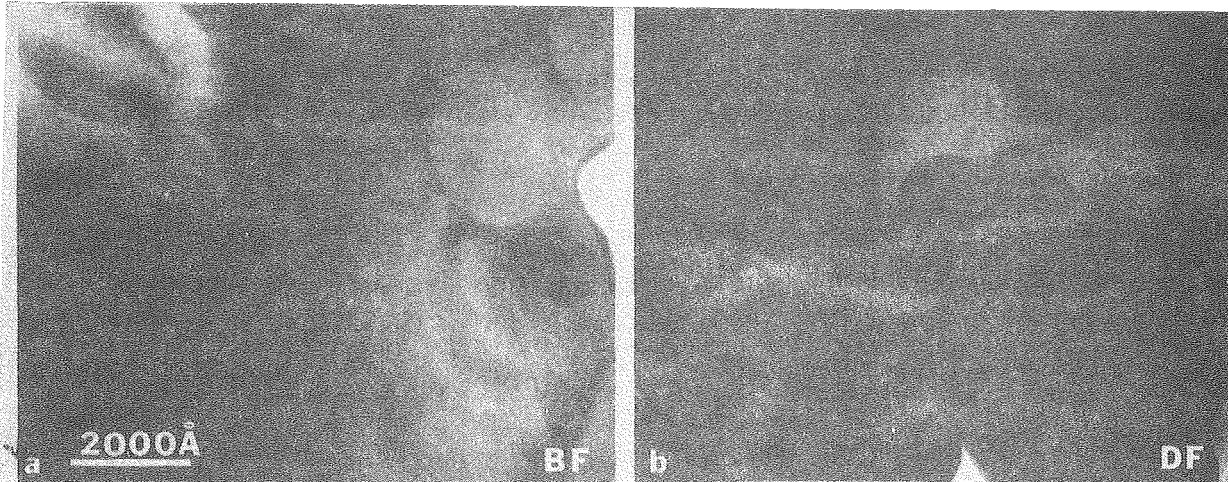


FIG. 8(a)

FIG. 8(b)

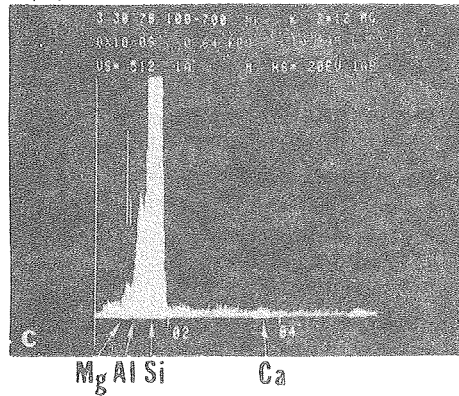


FIG. 8(c)

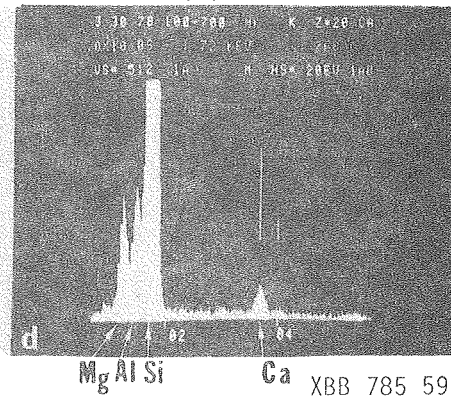


FIG. 8(d)

FIG. 8

- (a) Bright field showing ionisation damage in glassy phase
- (b) Dark field image using diffuse scattering from glassy phase
- (c) STEM X-ray analysis of a large area of Si_3N_4 . $\text{MgO} + \text{Al}_2\text{O}_3$ -fluxed sintered Si_3N_4 (Kyocera, Japan).
- (d) STEM X-ray analysis of glassy phase - notice impurities especially Ca

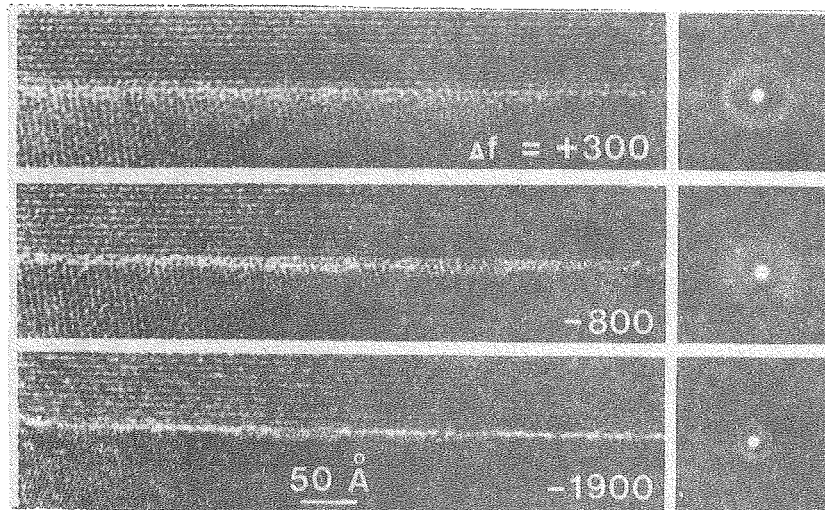


FIG. 9(a)

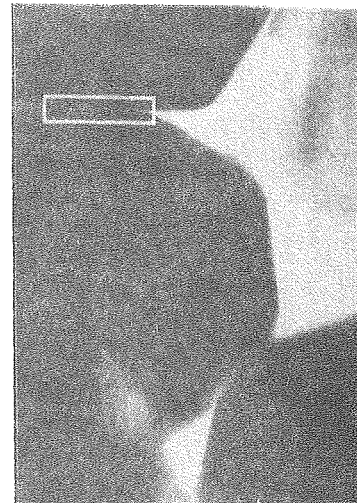


FIG. 9(b)

XBB 785 5932

FIG. 9

- (a) Through-focus-series of lattice images of a grain boundary in same material as Fig. 8. Middle image is at Scherzer focus.
- (b) Dark field image of the same boundary. (box corresponds to the area shown in (a)).

Electron microscopy has been used to characterize microsegregate defects in CGGG. High voltage electron microscopy (HVEM) has been used to investigate the structure, morphology, and crystallography of the segregates and their associated dislocations. HVEM permits the use of thicker ion-milled ceramic specimens and facilitates high-order BF and weak-beam DF imaging for improved resolution of these microstructural features.

Scanning transmission electron microscopy (STEM) with energy dispersive X-ray analysis (EDAX) has been used to determine the chemical composition of the segregates. Figure 12 shows the EDAX spectra obtained by placing a 200Å probe in each of the areas shown. Using this technique it was determined that the segregate region is depleted in germanium and rich in calcium and gallium relative to the $\text{Ca}_3\text{Ga}_2\text{Ge}_2\text{O}_{12}$ matrix. Since no evidence of other elements is observed, these defects result from microsegregation of elements intrinsic to the CGGG system.

4. Characterization by Lattice Imaging of "LMSC" Glassy Carbon¹⁴

Carbons made by the controlled pyrolysis of thermosetting resins are non-graphitizing as opposed to the soft carbons that graphitize when heat-treated to or above 2000°C. The structure and properties of the non-graphitizing carbons have been the subject of investigation of a large number of workers. Glassy carbon is a representative of the non-graphitizing class. X-ray analysis has not uniquely determined whether glassy carbon is amorphous or not. Consequently high resolution electron microscopy has been used to resolve the question concerning the true structure of the so called glassy carbon. Heidenreich, Hess and Ban¹⁰ were the first to utilize this powerful technique on carbon black. Since then Ban and Hess^{7,14}, and Jenkins, Kawamura and Ban¹² used lattice imaging to analyze glassy carbon prepared by a technique developed at Swansea while Phillips¹³ successfully lattice imaged glassy carbon made by Polycarbon of California. We have been investigating the microstructure and properties of glassy carbon made by the LMSC process.

In the phase contrast mode as shown in Fig. 13 an aperture was used to allow imaging of all spots on the 002 ring to occur. Thus lattice fringes corresponding to the (00.2) planes of graphite were obtained over large thin areas. Micrographs were taken slightly under focus. The lattice images show fringes but with no preferred orientation indicating the isotropic nature of glassy carbon. The fringe spacing is 3.4Å, and fringes are continuous usually over 50Å. The fringe pattern resembles the "Jenkins nightmare" model¹², and there are no definite crystallite boundaries. The layers show extensive bending and splitting; stacking disorders are also encountered. The thickness of each packet of layers and the distance of continuity of the fringes parallel to the layers correspond to the two crystallite dimensions conceived by the X-ray investigators. Selected area diffraction shows the absence of (hk.l) (h, k, ≠ 0) reflections indicating the turbostratic nature of the structure. The stacked layers bifurcate at places indicating that pores are enclosed among interweaving layers.

5. Summary and Conclusions

The advantages of high resolution electron diffraction and imaging have been revealed in a wide variety of metallic systems, providing insight into the mechanisms of such phase transformations as ordering, spinodal decomposition, grain boundary precipitation, and the martensitic reaction. Structural discontinuities in interphase interfaces (atomic plane ledges) and grain boundaries (plane matching defects) have been identified with high precision, and compositional variations on an atomic scale have been detected, including solute segregation within ~ 10Å of a grain boundary.

In the study of ceramics, primary effort has been directed toward the detection of thin intergranular films with notable success. Atomic dimension microledges have also been revealed in crystallization interfaces, polytype boundaries and transformation fronts, and compositional variations near grain boundaries have recently been recorded in lattice images of a Magnesium Sialon. It therefore appears that the technique holds equal promise for analysis of the fundamental mechanisms of crystallization, phase transformation, diffusion and solute segregation in ceramics as well as metallic alloy systems.

The work presented here represents some of the potential of high resolution methods



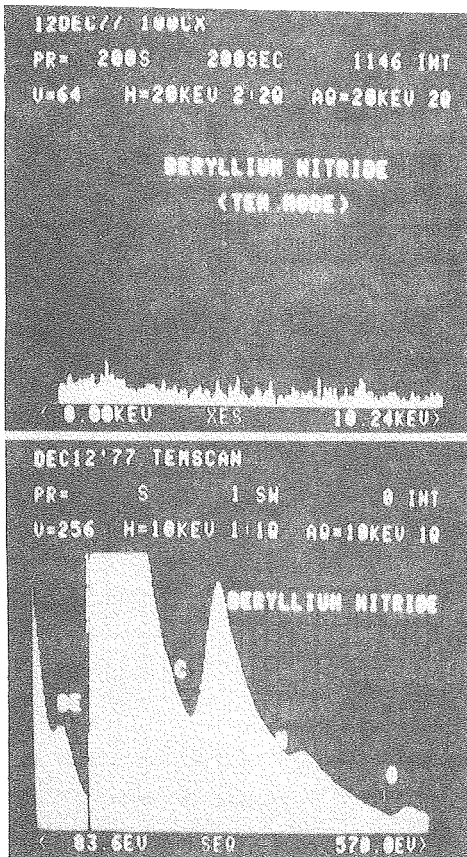
FIG. 10 (a) XBB 785 5934

FIG. 10(a)
Bright Field



FIG. 10(b) XBB 785 5934

FIG. 10(b)
Dark field image of hot-pressed Beryllium Sialon: No intergranular glassy phase is detected.



BBC 784 5308

FIG. 11

FIG. 11
A-ray STEM and ELS of specimen in Fig. 10 compared. The light elements are easily detected by ELS.

and is an initial step towards complete atomic characterization of materials. The most desirable progression of such research should lead to the attainment of structural images similar to those that are currently being used to explore the atomic arrangements in mineralogical specimens. This requires only a slight improvement in the contrast transfer characteristics of present day electron optics.

The resolution limit (Δx) determining the finest level of specimen detail which can be directly interpreted in terms of the atomic structure of a specimen is roughly given by:

$$\Delta x = 0.6 C_s^{1/4} \lambda^{3/4}$$

indicating that although some advantage will be realized by improved lens design (decreased C_s), much greater benefit will emerge from the attainment of stable, high accelerating voltages (decreased λ) in transmission electron microscopy. To avoid displacement damage an optimum voltage of 500 kV is suggested which will give a theoretical resolution of $\sim 1.7\text{\AA}$ point-to-point. Thus in the near future, high voltage, high resolution electron microscopy will make possible interpretable atomic resolution in inorganic materials, allowing direct visualization of the arrangement of atoms in solids. Once this capability has been achieved, it will be extremely useful to be able to identify the atoms comprising the imaged structure, uniquely and individually. Such a development must then be made the next goal in the dual microscopic-spectroscopic characterization of materials.

Acknowledgements

Financial support from the United States Department of Energy, Division of Basic Energy Sciences, through the Materials and Molecular Research Division of Lawrence Berkeley Laboratory and from the National Science Foundation is gratefully acknowledged. We are indebted to Dr. Roy Geiss (IBM San Jose), Dr. D. R. Clarke (N. American Rockwell) and Dr. Y. Yoda (Perkin-Elmer) for providing us time on their STEM instruments for microanalysis.

References

1. Fifth International Conference on High Voltage Electron Microscopy, Kyoto, Eds. T. Imura and H. Hashimoto) Japan Soc. Elec. Mic., Tokyo, Japan 1977.
2. G. Thomas in Physical Aspects of Electron Microscopy and Microbeam Analysis, Eds. B. M. Siegel and D. R. Beaman, Wiley & Sons, 1975, p. 81.
3. Symposium on Energy Loss and Electron Spectroscopy, Proc. EMSA 1977, (Claitor's Publishers, Baton Rouge), pp. 228-253.
4. R. Sinclair, R. Gronsky and G. Thomas, Acta Met. 24, 789, (1976).
5. B. V. N. Rao, J. Y. Koo and G. Thomas, Proc. EMSA, 1975, p. 30 see also G. Thomas, Met Trans. 9A, p. 439, (1978).
6. G. Thomas and B. V. N. Rao, International Conference on Martensitic Transformations, KIEV USSR (in press), LBL-6242.
7. R. Gronsky and G. Thomas, Scripta Met., 11, p. 791, (1977).
8. C. K. Wu, R. Sinclair and G. Thomas, Met. Trans., 9A, p. 381, (1978).
9. D. R. Clarke and G. Thomas, J. American Ceramics Society, 60, p. 461, (1977) *ibid.*, 61, p. 114, 1978.
10. R. D. Heidenreich, W. M. Hess and L. L. Ban, J. Applied Cryst. 1, 1, 1-19 (1968).
11. L. L. Ban and W. M. Hess, "Microstructures of Carbons: A High Resolution Microscopy Study", 10th International Biennial Conference on Carbon, Lehigh University, SS99, 161-162, (1971).

12. G. M. Jenkins, K. Kawamura, and L. L. Ban, Proc. Roy. Soc. (Lond) A327, 501-507 (1972).
13. V. A. Phillips, Metallography 6, 361-364 (1973).
14. S. Bose, U. Dahmen, R. H. Bragg and G. Thomas, J. Amer. Ceram. Soc., 61, 174 (1978).

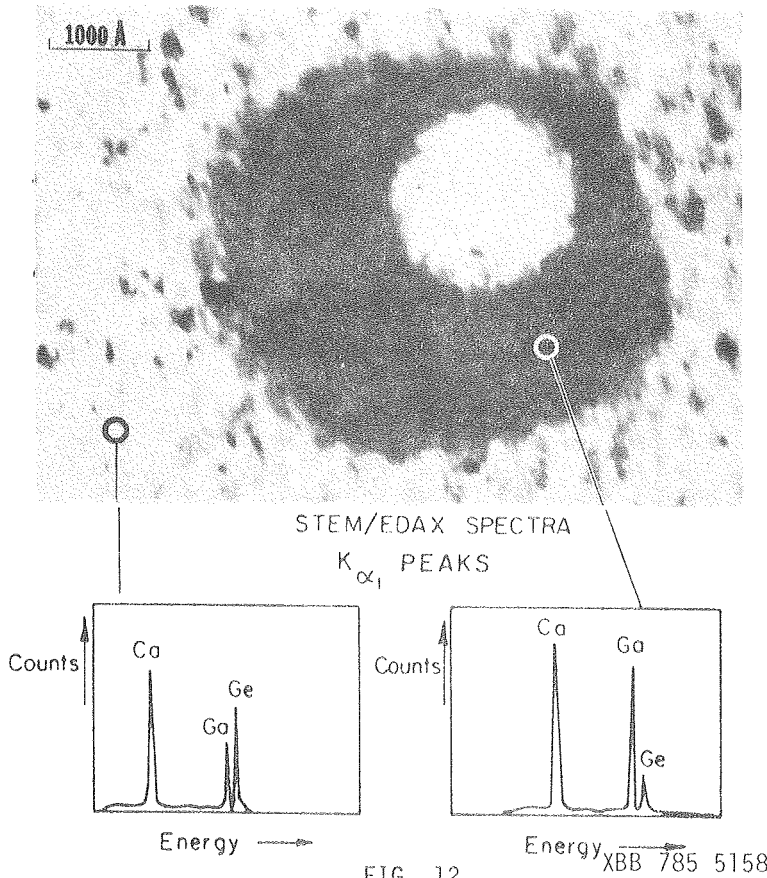


FIG. 12

650 kV Bright field high order image showing micro-segregation defect. Stereo-analysis showed that this is a spherical defect (hole or gas-filled cavity), surrounded by dark contrast. A 200Å probe was placed in each of the areas shown. The EDAX spectra obtained shows the defective region to be rich in Ca and Ga and depleted in Ge relative to the matrix material. Thus the defects occur due to microsegregation of elements intrinsic to the CGGG system. (Specimen courtesy of Phillips, Eindhoven).

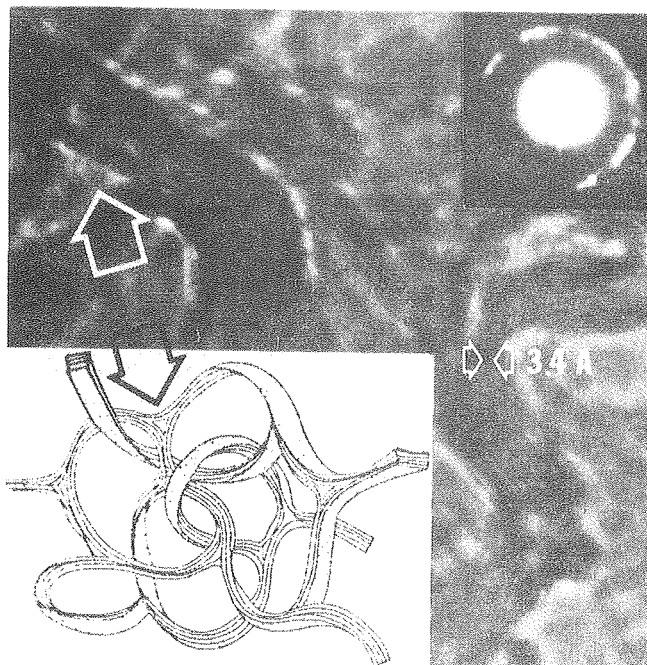


FIG. 13

Lattice image of glassy carbon showing isotropic distribution of interwoven fibers. The imaging condition is shown in the inset SAD. Note the spotty appearance of the 002 ring when a very small area is selected for diffraction.

The fibers are crystalline and tend to enclose very small pores at points of bifurcation (arrows), confirming Jenkins' "nightmare" model of glassy carbon (see sketch) and results obtained from small angle X-ray scattering.

FIG. 13

XBB 785-6028